PROCEEDINGS, 41st Workshop on Geothermal Reservoir Engineering
Stanford University, Stanford, California, February 22-24, 2016
SGP-TR-209

# Geodetic Measurements and Numerical Models of Deformation: Examples from Geothermal Fields in the Western United States

S. Tabrez Ali [1], John Akerley [2], Elena C. Baluyut [1], Nicholas C. Davatzes [3], Janice Lopeman [2], Joseph Moore [4], Mitchell Plummer [5], Paul Spielman [2], Ian Warren [6] and Kurt L. Feigl [1]

[1] University of Wisconsin, Madison, WI

[2] Ormat Technologies, Reno, NV

[3] Temple University, Philadelphia, PA

[4] University of Utah, Salt Lake City, UT

[5] Idaho National Lab, Idaho Falls, ID

[6] US Geothermal Inc., Boise, ID

E-mail: stali@geology.wisc.edu

**Keywords:** InSAR

## ABSTRACT

We use synthetic aperture radar (SAR) interferometry to measure time-dependent deformation at three actively producing geothermal fields in the Western United States. Raft River in Idaho, which began production in 2007 shows relatively rapid transient deformation which eventually decays to zero over a ~5 year interval. On the other hand, Coso in California, and Brady Hot Springs in Nevada, both of which have been producing for ~25 years, show gradual subsidence since at least 2004. We explore several different hypotheses for the processes driving deformation at the three sites, including poroelastic deformation due to injection/extraction of fluids and/or thermoelastic contraction due to cooling of rocks.

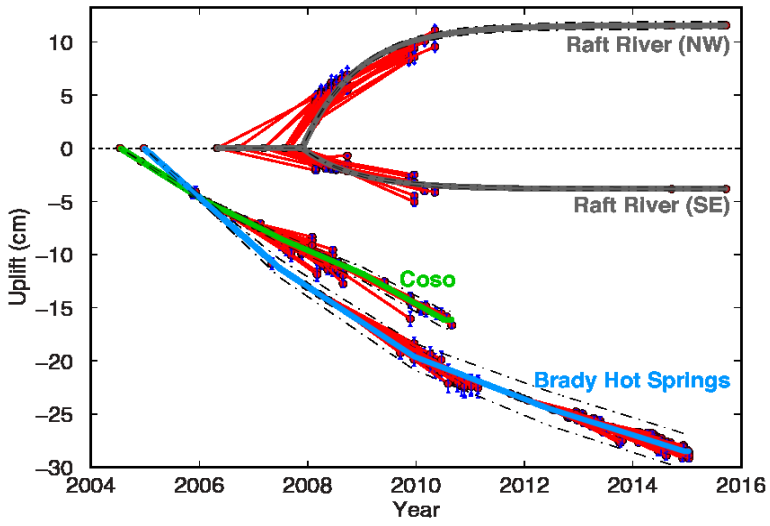


**Figure 1: Vertical displacement at Raft River, Coso, and Brady Hot Springs geothermal fields as a function of time, at a particular location, as estimated from individual InSAR pairs using temporal adjustment. The slope of each red colored line segment denotes the rate of vertical displacement for a single pair. A blue bar, drawn at the second epoch for each pair, denotes the uncertainty in the estimate.**

## 1. INTRODUCTION

Interferometric Synthetic Aperture Radar (InSAR) is an indispensable tool for measuring crustal deformation due to anthropogenic processes as it provides unsurpassed spatial sampling, very good precision, and a useful observation cadence. It has been used to measure deformation at a number of geothermal sites around the world (e.g., Ali et al., 2016 and references therein). However, the mechanism driving deformation is often poorly understood as geodetic observations have rarely been combined with calibrated reservoir models (e.g., Vasco et

al., 2013). By analyzing the temporal evolution and spatial pattern of the deformation, and combining them with numerical models, we can gain insight into associated subsurface processes, and the geometry of the reservoir(s). Here, we present preliminary results from three geothermal fields in Western United States where geothermal production has resulted in deformation.

**RAFT RIVER**

The Raft River geothermal field is located in Southern Idaho at the southern periphery of the Snake River plain, within the north-south trending Raft River valley. The valley is filled with ~1.5 km of pleistocene and tertiary sediments, conglomerates and volcanic rocks that overlie the precambrian basement. A ~13 MW power plant has been operational at Raft River since late 2007. The primary reservoir is within ~150 m thick, Elba quartzite, a fine grained metamorphosed quartz rich sandstone, just below the contact between the Salt Lake formation and the basement, between depths of 1400-1800 m (Bradford et al., 2013). Hot fluids are sourced from 4 producing wells at a depth of ~1500 m. Following generation of electricity, the fluids are recycled back via three injection wells located in the southeast corner of the field at a pressure of ~275 psi. The injection wells are ~1500 m deep, and cased to a depth of at least ~725 m. The rate of production and reinjection has roughly been constant at ~5000 gpm, since 2007. To measure deformation at Raft River, we analyze 33 SAR images acquired by the Envisat satellite, operated by the European Space Agency (ESA), and the TerraSAR-X satellite, operated by the German Space Agency (DLR). SAR interferograms at Raft River show no deformation prior to the start of production in 2007. However, deformation is observed in all coherent Envisat interferometric pairs spanning the production period. Figure 2 shows wrapped phase and unwrapped range change rate in mm/year for a single interferometric pair spanning the 2007.192-2008.246 time interval. Significant uplift (negative range change) is observed near the southeastern part of the field, where most of the injection wells are located. Subsidence (positive range change) is observed in an area west of, but adjacent to, the production wells. This signature is consistently observed in all Envisat interferometric pairs spanning the 2007-2011 time interval. Interferograms created using SAR data acquired by the TerraSAR-X satellite since 2014 do not show deformation in the area surrounding the wells. To gain insight into the trend of the deformation, we perform time series analysis using the procedure described in Ali et al. (2016). The results, i.e., uplift and subsidence over time, are shown at two locations (denoted by stars in Figure 2) in Figure 1. The trend (solid gray line in Figure 1) is zero deformation until start of production, followed by an exponentially decaying rate of uplift, and subsidence, respectively.

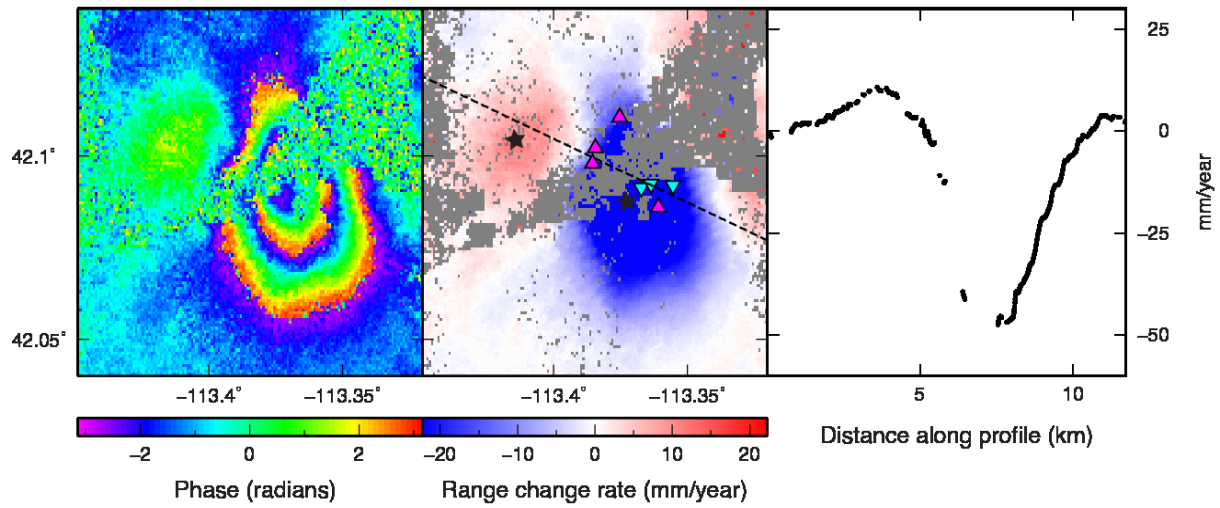


**Figure 2: Left: Observed wrapped phase values (in radians) over a ~1 year interval from 2007.192 - 2008.246. One colored fringe corresponds to one cycle of phase change or 28 mm of range change, towards or away from the satellite. Right: Range change rate in mm/year, calculated by unwrapping the observed wrapped phase shown in left. Blue color indicates decrease in range between the ground and the satellite and therefore represents uplift, whereas red color indicates increase in range and represents subsidence. Injection and production wells are represented by cyan and magenta triangles, respectively. Black stars represent the location at which uplift is plotted over time in Figure 1.**

Transient uplift at Raft River, centered near the injection wells, is not likely to be the result of thermoelastic effects because reinjection of cooler brine would decrease the temperature of the rocks. However, reinjection of fluids can cause transient uplift, due to poroelastic processes, which then decays over time as the system reaches steady state. To gain insight into the processes we use a simple, idealized, 2D poroelastic model, as shown in Figure 3 (top left). The horizons in this idealized model are based on the geology of the field (e.g., Ayling and Moore, 2013). The domain is 7.5 km long and 3 km deep. Two wells, separated by a distance of 3.5 km, are used to withdraw and reinject fluids at a constant rate. The fractured reservoir, with an assumed Young's modulus of 3.0E10 GPa, is represented by a 200-m-thick layer between the Salt Lake formation (above), and the basement (below), both of which are assumed to be relatively impermeable (i.e., K=1E-20 $m^2$). We solve the quasi-static linear poroelasticity problem using Defmod (Ali, 2014), a parallel, unstructured finite element code for modeling crustal deformation. The simulation is run for a period of 8 years with a time step of 58 days. We find that a reservoir scale permeability of 3.75E-15 $m^2$ results in an uplift rate that matches the observed uplift rate quite well. However, the total increase in maximum pressure at steady state is relatively high, i.e., ~10 MPa which suggests that the volume of the reservoir is much larger. If we increase the reservoir thickness to 1000 m, by making the layers above the reservoir permeable, then we get similar uplift rates although at a much lower pressure, i.e., 1.75E6 Pa or ~250 psi which is less than or equal to the injection pressure. Alternatively, we could decrease the modeled moduli of the rocks in the reservoir by the factor of 5, although such low values are physically implausible. These calculations demonstrate the tradeoff between the effective size of the reservoir, its effective elastic moduli, change in pressure over time, and surface deformation. We would also like to point that, unlike InSAR observations, the magnitude of uplift, and subsidence predicted by our model is the same suggesting that lateral heterogeneities, either in the moduli, or permeability, or the geometry of the reservoir, play a key role as well.

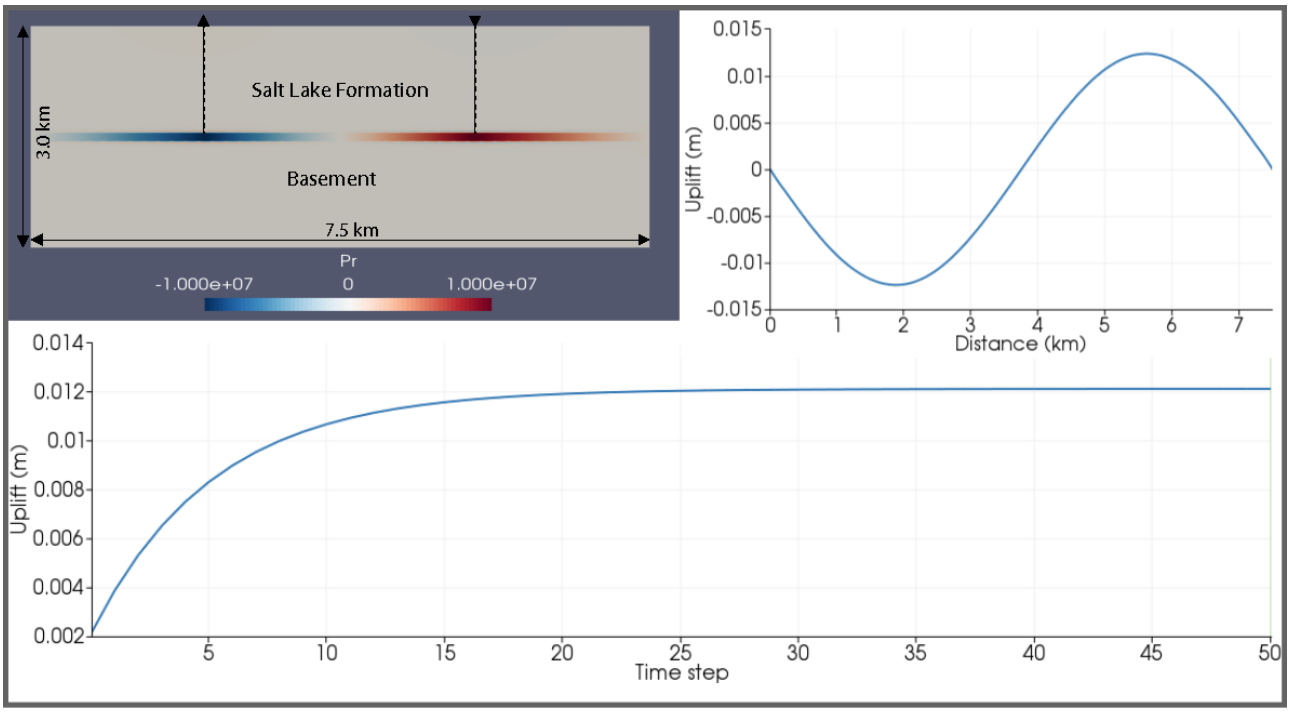


**Figure 3: Top left: 2D, poroelastic model showing pressure distribution (in Pa) at steady state. Top right: Cumulative uplift at surface at the end of the simulation. Bottom: Uplift as a function of time near the injection well at the surface (inverted triangle in the Figure shown in top left).**

## COSO

The Coso geothermal field, located east of the Sierra Nevada near China Lake, is the third largest geothermal field in the United States with an installed capacity of ~270 MW. Four geothermal plants have been producing electricity since 1990 from the reservoir where fluid temperatures reach ~350 deg C at relatively shallow depths of ~3 km. The reservoir at Coso is within highly fractured plutonic and metamorphic rocks of Mesozoic

age (Monastero et al., 2005). Approximately 100 production wells extract fluids, which, following the generation of electricity and condensation, are reinjected via 30-40 injection wells located within or near the field.

Fialko and Simons (2000) analyzed SAR data acquired between 1993 and 1999 by the ERS-1 and ERS-2 satellites operated by ESA to characterize deformation at Coso. Their results show a complex deformation pattern spread over a 50 $km^2$ area with peak subsidence rates of the order of ~3.5 cm/year. Using elastic models consisting of pressurized spheroidal cavities, they estimate that a ~6.5 km long and ~1.5 km wide contracting source, located at a depth of ~2.5 km can explain most of the deformation observed in the interferograms. Here, we used SAR data acquired by the Envisat satellite, also operated by ESA, to form 32 interferometric pairs in order to characterize the spatio-temporal evolution of deformation over the 2004-2011 time interval. Figure 4 shows result from single interferogram spanning the 2008.183-2009.906 time interval. A large circular interference pattern, associated with subsidence, is observed over a 100 $km^2$ area. This signature is consistently observed in all interferometric pairs spanning the 2004-2011 time period. We perform time series analysis using the same procedure described above. The result, i.e., uplift at a single location, denoted by the star in Figure 4, is shown in Figure 1. The trend (in solid green) is almost linear over the time interval of observation, suggesting that the driving processes have reached a steady state at Coso.

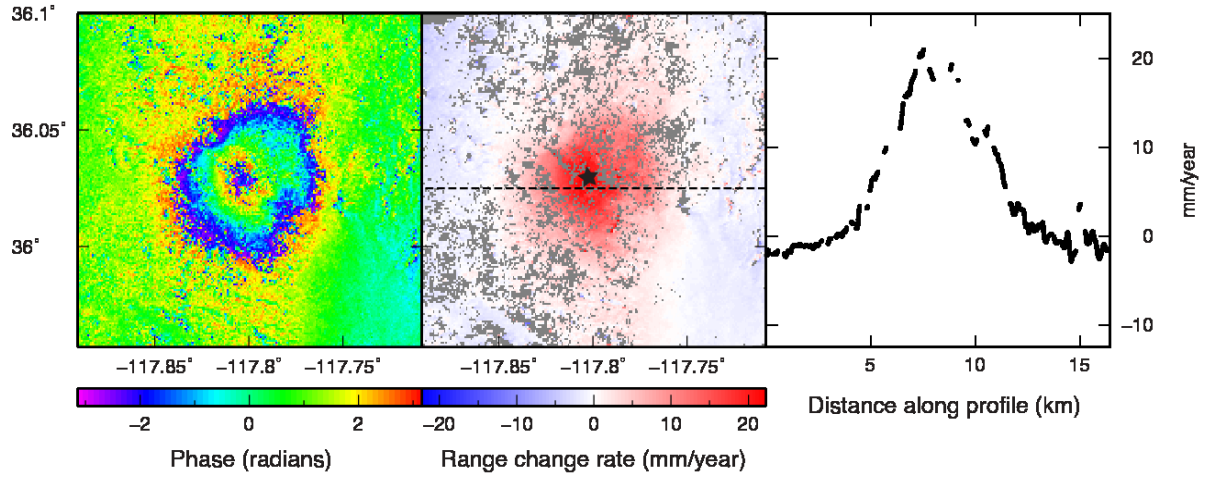


**Figure 4: Observed wrapped phase and range change rate at Coso, over ~1.7 years spanning the 2008.183 - 2009.906 time interval. Plotting conventions are same as those in Figure 2.**

In order to gain insight into the underlying mechanism, we perform inverse modeling using poroelastic as well as thermoelastic models. We solve the coupled deformation diffusion problem using the finite element code Defmod (Ali, 2014). To solve the inverse problem we use a gradient based inversion scheme similar to the one described in Ali et al. (2014). Following Fialko and Simons (2000), we parameterize the geometry of the reservoir using an ellipsoid (oblate spheroid) which in our case deforms due to changes in pressure or temperature. We assume a relatively low Young's modulus of 25 GPa (uniform throughout the model domain), and run the simulation until the system reaches steady state, i.e., the rate of deformation becomes constant. Loading can be specified either by imposing a flow rate, or by specifying pressure change. Because net flow, in or out of the reservoir, is difficult to constrain as natural recharge is often unknown, we use impose a pressure boundary condition at a single node at the center of the reservoir. We assume that pressure drops at a rate of 0.333 MPa/year, which is equivalent to ~33.3 m drop in head, per year. The free parameters in our model include, the location of the reservoir, and the length of its major and minor axes. The modeled rate of range change, at steady state, is shown in Figure 5b, along with the average range change rate calculated by stacking all the interferometric pairs (Figure 5a). The optimized model requires a reservoir that is ~4 km thick, ~6 km long by ~6 km wide, and centered at depth of 2.4 km, as shown in Figure 5 (bottom panel). To a first order, our model matches the InSAR observations quite well. Figure 5 also shows the uplift as well as the pressure change required per year to cause the observed deformation, superimposed on the mesh used for the analysis. Under this scenario the pressure within the confined reservoir has to continually decline over time. If, on the other

hand, we assume that all deformation is due to thermoelastic contraction, due to cooling of reservoir, then, a temperature change of ~3.33 deg C per year throughout the reservoir (assuming a thermal expansion coefficient of 1.0E-5) can explain the observations equally well. Under this scenario, the (fractured) reservoir rock cools uniformly, as the temperature of fluids in the reservoir declines over time. Irrespective of the mechanism of deformation our results highlight the importance of InSAR observations in calibrating reservoir models.

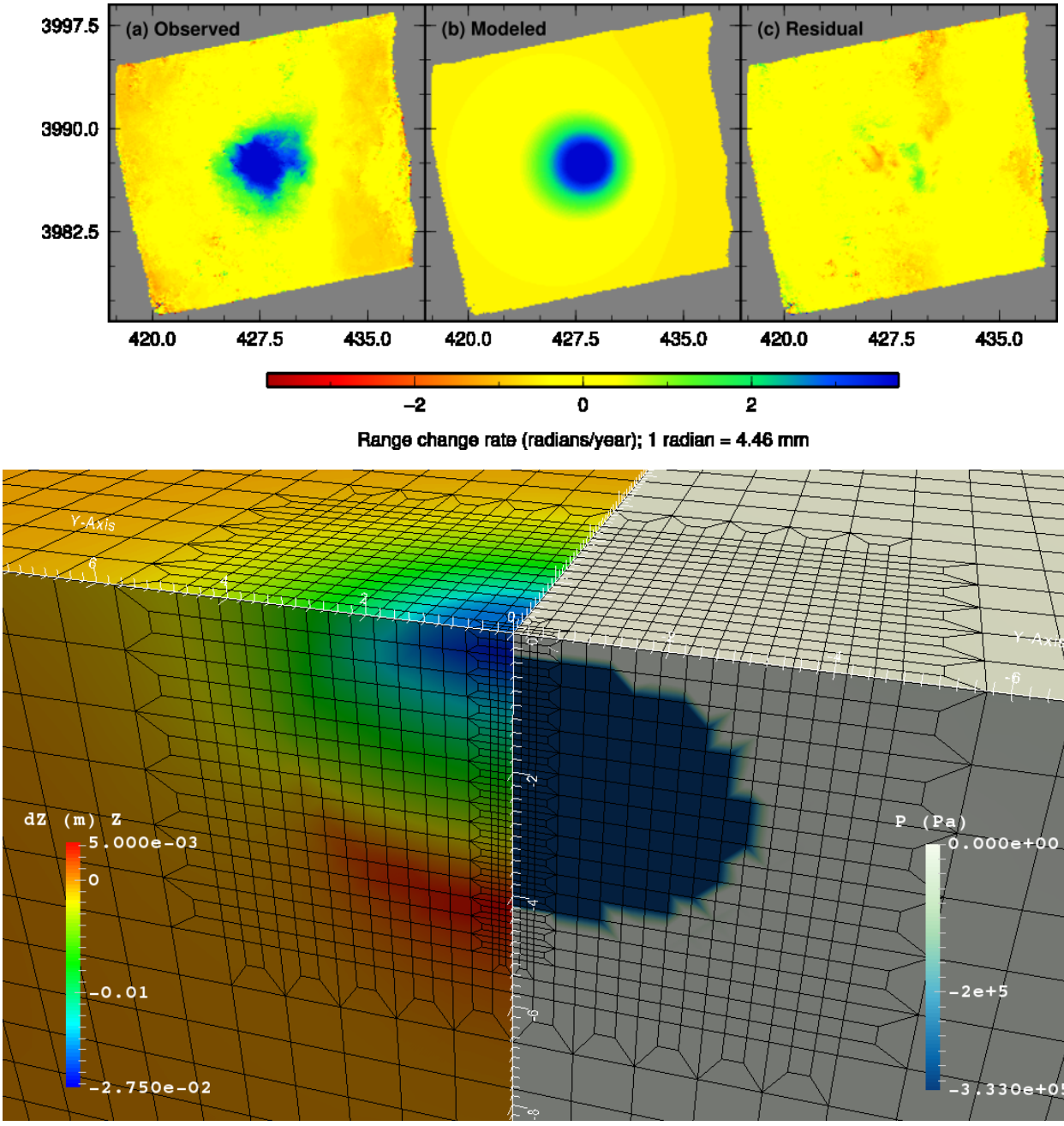


**Figure 5: Top: (a) Observed range rate calculated by stacking 32 interferometric pairs; (b) Modeled range change rate calculated using parameters estimated from inverse modeling; (c) Residual range change rate calculated by subtracting the modeled values from the observed values. Bottom: Subsidence and pressure change in Pa (per year), at steady state, along with the mesh used for the modeling.**

## BRADY HOT SPRINGS

The Brady Hot Springs geothermal field is located near the Hot Spring Mountains in Northwestern Nevada, approximately 80 km east-northeast of Reno. A ~15 MW geothermal plant at Brady has been generating power

since 1992. Hot fluids are withdrawn using six production wells (only five are currently operational) from depths of 400-1850 m and recycled back into the subsurface, between depths of 200 and 300 m, via two injection wells, located 1500 to 2500 m away in the north-northeast direction. The geothermal reservoir is hosted in layered Tertiary volcanic rocks, including welded tuff, rhyolite and meta-sediments overlying Mesozoic crystalline intrusions (Jolie et al., 2012, Siler and Faulds, 2013). Oppliger et al. (2004, 2006) used InSAR to characterize deformation resulting from geothermal production between 1997 and 2002, using SAR data acquired by ERS satellites operated by ESA, and interpreted the deformation in terms of a contracting aquifer. More recently, Ali et al. (2016), used multiple images acquired between 2004 and 2014 by several satellites, including ERS-2 and Envisat, operated by ESA, ALOS, operated by Japanese space agency (JAXA) and TerraSAR-X and TanDEM-X, operated by DLR, to measure and characterize the time-dependent deformation at Brady. Figure 6 shows observed phase, and range change rate, over a 308-day time interval between Dec-24-2011 and Oct-27-2012 from a single TerraSAR-X interferometric pair. Results from time series analysis, i.e., uplift at a single location, denoted by the star in Figure 6, are shown in Figure 1 (in solid blue). Unlike Coso, where subsidence is observed over a large area, subsidence at Brady is observed at multiple locations. A large ellipsoidal shaped bowl of subsidence is observed near the production wells, in the southern part of the field. Localized subsidence is also observed near the two injection wells towards the northeast. At Brady, we do not find any evidence of drop in the water level over the 2004-2016 time interval. This suggests that subsidence is unlikely due to pore pressure changes. On the other hand, reinjection of cooler brine can cause the rocks in the shallow subsurface, i.e., between 100-500 m, to cool over time. Lateral heterogeneities in material properties and differences in the fracture density can result in localized cooling which could potentially explain some of observations.

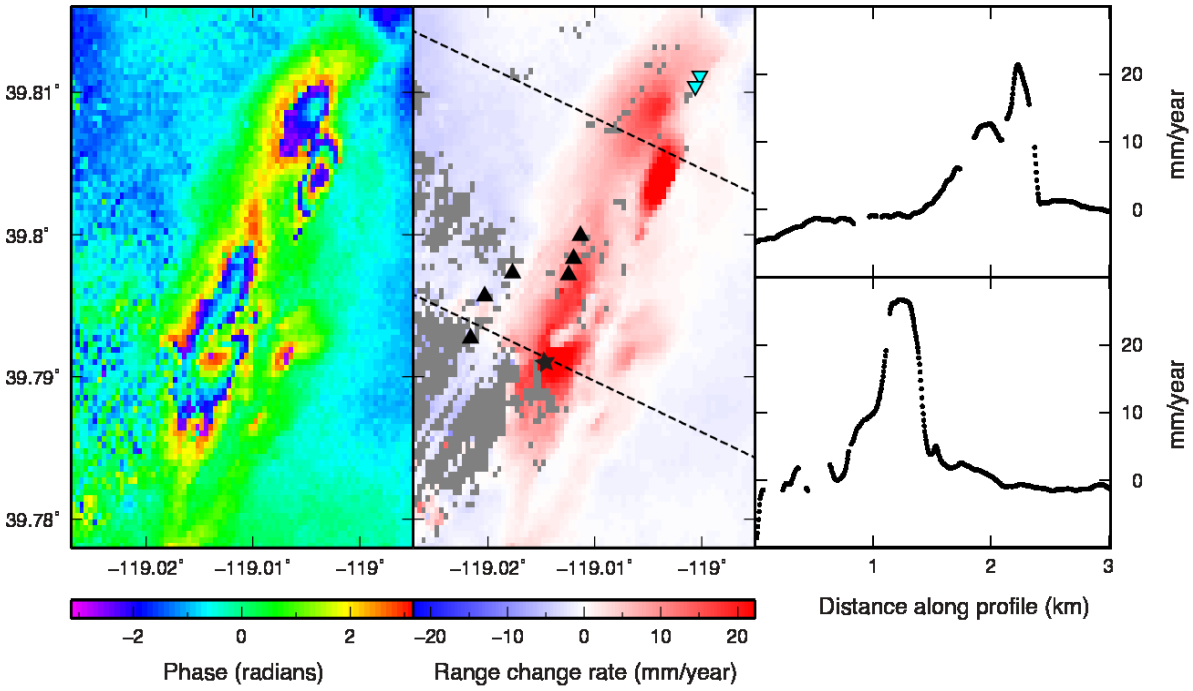


**Figure 6: Observed wrapped phase and range change rate at Brady Hot Springs, over ~0.85 years spanning the 2011-12-24 - 2012-10-27 time interval. Plotting conventions are same as those in Figure 2. Production wells are shown in black triangles. Injection wells are represented as cyan colored inverted triangles.**

**ACKNOWLEDGEMENTS**

Raw SAR data from the ERS and Envisat satellite missions, operated by the European Space Agency (ESA) are copyrighted by ESA and were provided through the WInSAR consortium at the UNAVCO facility. SAR data from the ALOS satellite mission operated by the Japanese Space Agency (JAXA) were acquired from NASA's Distributed Active Archive Center at the Alaska Satellite Facility (ASF). SAR data from the TerraSAR-X and

TanDEM-X satellite missions operated by the German Space Agency (DLR) were acquired through Research Project RES1236. All interferograms were created using the GMTSAR InSAR processing system (Sandwell et. al, 2011). This research was supported by grants DE-EE0005510 and DE-EE0006760 from the Geothermal Technologies Office of the U.S. Department of Energy. Elena C. Baluyut was supported by the National Science Foundation Graduate Research Fellowship under grant DGE-1256259.

**REFERENCES**

Ali, S.T., 2014. Defmod-Parallel multiphysics finite element code for modeling crustal deformation during the earthquake/rifting cycle. arXiv preprint arXiv:1402.0429.

Ali, S.T., Feigl, K.L., Carr, B.B., Masterlark, T. and Sigmundsson, F., 2014. Geodetic measurements and numerical models of rifting in Northern Iceland for 1993–2008. Geophysical Journal International, 196(3), pp.1267-1280.

Ali S.T., Akerley J., Baluyut E.C., Cardiff M., Davatzes N.C., Feigl K.L., Foxall W., Fratta D., Mellors R.J., Spielman P., Wang H.F. and Zemach E., Time-series analysis of surface deformation at Brady Hot Springs geothermal field (Nevada) using interferometric synthetic aperture radar, Geothermics, 61, pp.114-120,

Ayling, B. and Moore, J., 2013. Fluid geochemistry at the Raft River geothermal field, Idaho, USA: New data and hydrogeological implications. Geothermics, 47, pp.116-126.

Bradford, J., McLennan, J., Moore, J., Glasby, D., Waters, D., Kruwell, R., Bailey, A., Rickard, W., Bloomfield, K. and King, D., 2013, February. Recent developments at the Raft River geothermal field. In Proceedings, Thirty-Eighth Workshop on Geothermal Reservoir Engineering, Stanford University, Stanford, California.

Fialko, Y. and Simons, M., 2000. Deformation and seismicity in the Coso geothermal area, Inyo County, California: Observations and modeling using satellite radar interferometry. Journal of Geophysical Research B, 105(B9), pp.21781-21793.

Jolie, E., Faulds, J. and Moeck, I., 2012. The Development of a 3D Structural-Geological Model as Part of the geothermal Exploration Strategy–A Case Study From the Brady's Geothermal System, Nevada, USA. In Proceedings, 37th Workshop on Geothermal Reservoir Engineering. Stanford University, Stanford, California, January 30-February 1.

Monastero, F.C., Katzenstein, A.M., Miller, J.S., Unruh, J.R., Adams, M.C. and Richards-Dinger, K., 2005. The Coso geothermal field: A nascent metamorphic core complex. Geological Society of America Bulletin, 117(11-12), pp.1534-1553.

Oppliger, G., Coolbaugh, M., Shevenell, L. and Taranik, J., 2005. Elucidating deep reservoir geometry and lateral outflow through 3-D elastostatic modeling of satellite radar (InSAR) observed surface deformations: an example from the Bradys geothermal field. Geothermal Resources Council Transactions, 29, pp.419-424.

Oppliger, G., Coolbaugh, M. and Shevenell, L., 2006. Improved visualization of satellite radar InSAR observed structural controls at producing geothermal fields using modeled horizontal surface displacements. Geotherm. Res. Counc. Trans., 30, pp.927-930.

Sandwell, D., Mellors, R., Tong, X., Wei, M. and Wessel, P., 2011. Open radar interferometry software for mapping surface deformation. EOS, Transactions American Geophysical Union, 92(28), pp.234-234.

Siler, D.L. and Faulds, J.E., 2013. Three-Dimensional Geothermal Fairway Mapping: Examples from the Western Great Basin, USA. Geothermal Resources Council Transactions, pp.327-332.

Vasco, D.W., Rutqvist, J., Ferretti, A., Rucci, A., Bellotti, F., Dobson, P., Oldenburg, C., Garcia, J., Walters, M. and Hartline, C., 2013. Monitoring deformation at the Geysers Geothermal Field, California using C- band and X- band interferometric synthetic aperture radar. Geophysical Research Letters, 40(11), pp.2567-2572.